

We are IntechOpen, the world's leading publisher of Open Access books Built by scientists, for scientists

4,800

Open access books available

122,000

International authors and editors

135M

Downloads

Our authors are among the

154

Countries delivered to

TOP 1%

most cited scientists

12.2%

Contributors from top 500 universities



WEB OF SCIENCE™

Selection of our books indexed in the Book Citation Index
in Web of Science™ Core Collection (BKCI)

Interested in publishing with us?
Contact book.department@intechopen.com

Numbers displayed above are based on latest data collected.
For more information visit www.intechopen.com



Selective Mono-Hydrogenation of Polyunsaturated Hydrocarbons: Traditional and Nanoscale Catalysis

Ting-An Chen and Young-Seok Shon

Abstract

Selective hydrogenation of olefins is an important process in both chemical and pharmaceutical industries. This chapter reviews intriguing catalytic studies accomplished by employing a variety of catalysts such as metal complexes, supported materials, supported metal complexes, and nanosized materials for polyene hydrogenation. In addition, new research area involving unsupported colloidal nanoparticle catalysts, which exhibit an excellent activity and selectivity toward the polyene hydrogenation is introduced. The high activity of colloidal metal nanoparticle catalysts often allows the reactions to be completed under mild conditions, at atmospheric pressure, and room temperature. These colloidal nanoparticle catalysts also offer an advantage of facile separation and multiple recycling without significant losses in activity and selectivity. This chapter provides important fundamental understandings on the influence of chemical environments (solvents, ligands, dopants, etc.) and compositions (metal complex, metals, alloys, etc.) toward the catalytic activity and selectivity of various catalysts in homogeneous, heterogeneous, and semi-heterogeneous conditions. The systematic evaluation discussed in this chapter would pave a way to further develop chemo-, regio-, and stereo-selective catalysts for polyene hydrogenation.

Keywords: selective hydrogenation, catalysis, nanocatalysis, homogeneous, heterogeneous, semi-heterogeneous

1. Introduction

Selective hydrogenation of polyunsaturated hydrocarbons including polyenes and alkynes are vitally important processes in fine chemical industries [1]. For instance, polymerization and hydroformylation reactions require a high purity of monomeric alkenes. However, light alkenes produced by catalytic cracking of petroleum often contain a high level of dienes or alkynes, making the selective hydrogenation of these compounds to monoenes in the presence of alkenes that are highly essential [2]. The removal of polyunsaturated hydrocarbons is also often important for catalysis applications, since their strong adsorption to metal surfaces would deactivate the catalyst during the reaction. In addition, the unique scent of natural polyunsaturated compounds makes them an important ingredient in

perfume industry and more attentions are currently placed on the single hydrogenation products of the natural triene substrates as both perfume ingredients and pharmaceutical precursors [3, 4]. Many efforts have been carried out in the past for selective hydrogenation using either homogenous molecular catalysis or heterogeneous solid state reactions [5, 6]. With both the pros and cons of each approach, the semi-heterogeneous characteristics of soluble colloidal metal nanoparticles in addition to their large surface area to volume ratio have increased research interests on nanoparticle catalysts for selective organic reactions. This chapter reviews the up-to-date progress on the selective hydrogenation of polyunsaturated olefins using both traditional and nanoscale catalysts.

2. Traditional catalysts

2.1 Metal complexes for hydrogenation of dienes in homogeneous system

Homogeneous system using metal complex usually exhibits high reactivity for the catalytic hydrogenation of dienes [7, 8]. Schrock et al. proposed the reaction mechanism for the catalysis of homogeneous rhodium metal complex ($[\text{RhL}_n]^+$) that is efficient for the selective hydrogenation of norbornadiene (NBD). Based on the results of 1a–1d in **Table 1**, the diene reaction rate was not significantly affected by the addition of other reagents. **Table 1** also presents the effect of the size of the ligand on metal complex (R_{ene} values of 1a, 2, and 3 in **Table 1**). These results indicated that the reactivity decreases as the size of the ligand increases. This phenomenon is similar to other homogenous reactions of metal complex. Dienes could effectively chelate to the metal complex and form strong bonds with metal atoms, even under the presence of excess hydrogen gas. The strong bond formation between metal ion and diene could be visualized by the rapid color change of the complex after diene was added to the solution. The overall results indicated that the major path involves the coordination of olefins and the adsorption of hydrogen ($[\text{RhH}_2(\text{NBD})\text{L}_n]^+$), which are followed by the addition of hydride to form Rh-alkyl intermediate ($[\text{RhH}(\text{NBD-H})\text{L}_n]^+$). After the reductive elimination of alkyl and hydride, rhodium metal complex ($[\text{RhL}_n]^+$) is regenerated and is ready for recycle. The deuterium gas addition study for $[\text{Rh}(\text{NBD})\text{L}_n]^+$ revealed that the substrate is chelated on metal ion by the two π bonds. Therefore, the primary hydrogenation reaction would have two deuterium on the endo side of the norbornene.

Run	Catalyst	R_{diene}	R_{ene}	Max % ene
1a	$[\text{Rh}(\text{NBD})(\text{PPh}_3)_2]^+\text{PF}_6^-$	0.22	0.03	97
1b	1a with 3.0 mol of HClO_4	0.21	0.05	92
1c	1a with D_2	0.22	(b)	(b)
1d	1a with 2.0 mol of Et_3N and D_2	~ 0.21 (initial) ^a	(b)	80
2	$[\text{Rh}(\text{NBD})(\text{PPh}_2\text{Me})_2]^+\text{PF}_6^-$	0.16	0.12	97
3 ^b	$[\text{Rh}(\text{NBD})(\text{PPhMe}_2)_2]^+\text{PF}_6^-$	0.14	0.19	90

^aA markedly nonlinear rate was observed. The behavior was more nearly first order in olefin ($k = 4.4 \times 10^{-4} \text{s}^{-1}$).

^bCatalyst precursor = 0.053 mmol.

Data reproduced from [7].

Table 1.

The hydrogenation of norbornadiene in acetone with Rh complex (in 10.0 ml of acetone, 1.0 ml of NBD, $30.0 \pm 0.5^\circ\text{C}$, 1 atm total pressure of H_2 , 0.026 mmol of catalyst precursor, R = rate in mmol/min).

The metal complex catalyst could also be deactivated once two bonds on dienes are chelated to one metal ion. Because the metal ion with a chelated diene compound is too stable to react, the bidentate ligand as shown in **Figure 1** was essential in avoiding this deactivation by diene coordination. The catalysis results of substituted dienes by the rhodium complex with different ligands showed the influence of ligands on the catalytic selectivity for 1,2- and 1,4-addition products. The comparisons of results indicated that diphos and arphos favor the 1,4-addition product (80–90%), while dpea favors the 1,2-addition product (~80%). Between diphos and arphos, arphos exhibits slightly higher selectivity toward the 1,4-addition product. The catalytic reaction of 1,4-cyclohexadiene begins with the isomerization to 1,3-cyclohexadiene. The produced 1,3-cyclohexadiene, however, would not dissociate from the metal ion, forming $[\text{Rh}(\text{diene})\text{L}_n]^+$, due to the strong bond formation between metal ion and diene compound. The monoene compound would dissociate from metal ion after its formation, because it forms a weakened bond with metal ion. The high conversion yields (>98%) of these catalytic reactions indicated the high reactivity of the $[\text{Rh}(\text{diene})\text{L}_n]^+$ catalyst in general.

Frankel et al. showed that other metal complex catalysts such as chromium complex, methyl benzoate- $\text{Cr}(\text{CO})_3$, also favors the 1,4-addition reduction of dienes for the hydrogenation of 1,3- and 2,4-hexadiene (70–90%) [8]. In contrast, the formation of 1,4-addition hexene product was accompanied with the major formation of conjugated 1,3- and 2,4-diene products for the catalytic hydrogenation of 1,4- and 1,5-hexadiene indicating that the reaction would most likely involves the first isomerization of isolated dienes to conjugated intermediates. The catalytic reactions of conjugated dienes with methyl substituted group(s) also mostly produced the 1,4-addition hydrogenation products as shown in **Table 2**. The position of substituted methyl group would not have a major effect on the catalytic activity except the case for 2,5-dimethyl-2,4-hexadiene, which exhibits low reactivity due to the large steric interference of four methyl groups. The difficulty in generating the product with cis-conformation, which chromium complex catalyst favors, is considered to be the main reason. The 1,2-addition hydrogenation product generated from the catalytic reaction of 4-methyl-1,3-pentadiene is also turned out to be the 1,4-addition product involving H shift. The isomerization of 1,4-cyclohexadiene was also more favorable than the 1,4-addition hydrogenation, forming 1,3-cyclohexadiene as the major product. This result also proves that the isomerization would take place prior to the hydrogenation. When the reaction temperature is increased to 170°C, the hydrogenation product becomes the major (thermodynamic) product. The high stability of 1,3-cyclooctadiene also reduces the reactivity

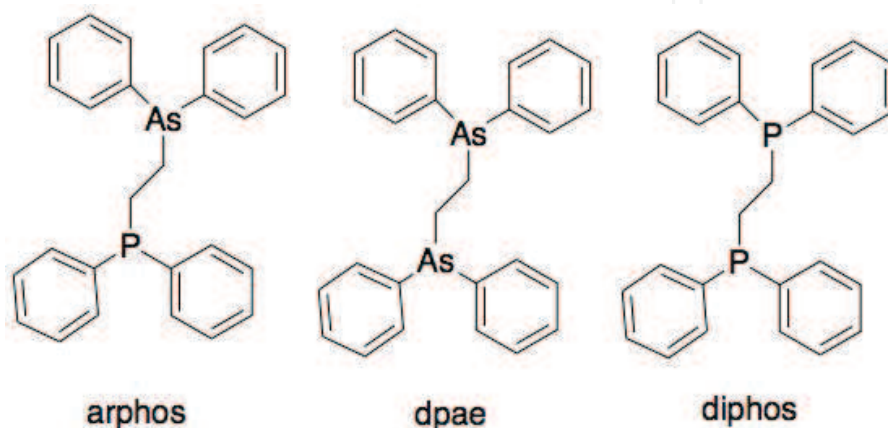


Figure 1.
Different bidentate ligands for diene catalysis reaction by rhodium complex [7].

of substrate at the lower temperature resulting in low yield for the hydrogenation product.

Regioselective asymmetric monohydrogenation of 1,4-dienes has been studied using various organometallic catalysts including ruthenium, rhodium, and iridium complexes with N or P binding chiral ligands [9–12]. The iridium catalysts exhibited excellent enantioselectivity for the hydrogenation of disubstituted cyclohexadienes as shown in **Figure 2** below [12]. The catalytic reactions produced mono-hydrogenation products shown below as major products in the yields ranging from 45 to 99% depending on the structure of O-R group. Tetrahydropyranyl acetal (THP) and triisopropyl silyl ether (TIP) resulted in 99% monohydrogenation selectivity. The enantioselectivity of these two groups were 83 and 97%ee, respectively, indicating highly efficient regio- and enantioselectivity of Ir catalyst for the synthesis of silyl protected enol ethers. Oxidation of these chiral enol ethers led to the corresponding chiral α,β -unsaturated ketones.

Dienes, 9.5 mmol	k, h ⁻¹	Products (% at 6 h)			
	0.69				
	0.64				
	1.1				
	0.007				
	0.1 ^b				

^b At 175°C.

Data reproduced from [8].

Table 2.

Catalytic hydrogenation of methyl-substituted dienes with 0.5 mmol chromium complex (solvent: *n*-pentane, 50 ml; temperature: 160 °C; initial H₂ pressure: 30 atm.).

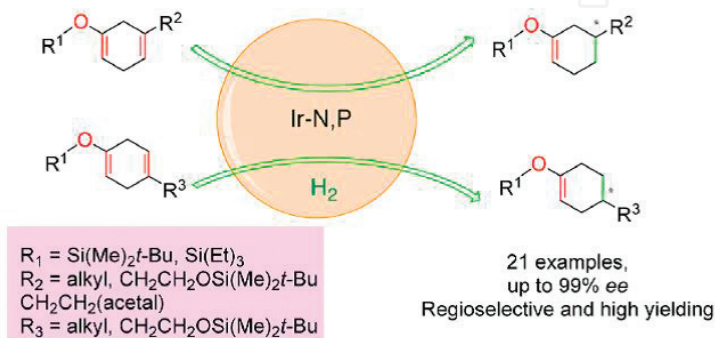


Figure 2.

Asymmetric hydrogenation using iridium metal complex (0.5 mol% Ir catalyst, PhCF₃, K₃PO₄, H₂, rt., 12 h). Reproduced from [12] with permission from the American Chemical Society.

2.2 Supported materials for the hydrogenation of dienes in heterogeneous system

In terms of reactivity, heterogeneous catalysts are usually less reactive than homogeneous systems. However, heterogeneous catalysts only require simple separation processes for purification and can be more easily recycled compared to homogeneous catalysts. Therefore, many research groups have been working on advancing fundamental understanding on the structure/property relationship and technological applications of heterogeneous catalysts in the past decade. Many of these supported metal catalysts are in fact in nanoscale dimensions, but many earlier catalysis studies did not attempt detailed characterizations on material sizes and their distributions on the supports. Both materials with and without well-defined sizes and structures including the catalysts reported as nanoparticulate materials are discussed here as traditional catalysts.

2.2.1 Supported metal catalysts: different strategies to modify activity

Selective hydrogenation of 1,3-butadiene was studied using graphite-supported palladium and platinum and the influence of FeCe alloying to these heterogeneous catalysts was investigated [13]. The results showed that the mono-hydrogenation and subsequent isomerization to 2-butene takes better place when the alloying was limited to less than 1/20 (**Figure 3**). The monohydrogenation selectivity was ascribed to the depletion of hydrogen atoms away from palladium surfaces by spill over to alloyed metal surfaces. The overall catalytic activity has also been increased by alloying of FeCe to Pd or Pt catalysts, indicating the activation of FeCe by spill over hydrogen.

Similarly, alumina-supported palladium catalysts doped with either tin or silver were tested for the selective hydrogenation of 1,5-hexadiene and 1,3-hexadiene [14]. Palladium on alumina itself produced mono-hydrogenation products from both 1,5-hexadiene and 1,3-hexadiene with a high selectivity even at full conversions. However, the selectivity for 1-hexene (or 3-hexene from 1,3-hexadiene) over the isomerized 2-hexene (trans > cis) from 1,5-hexadiene started to decrease at conversions higher than 80%. The addition of tin or silver tends to significantly increase the selectivity for 1-hexene, but with the loss of overall activity for mono-hydrogenation. This indicated that the addition of doping metal causes a geometric dilution of active Pd adsorption sites for both double-bond isomerization and hydrogenation.

Sulfidation of supported Pd catalysts has also been identified as an efficient way to increase the selectivity for mono-hydrogenation of dienes [15]. Supported palladium sulfide catalysts could be prepared by the addition of H₂S or Na₂S or the treatment with fuming sulfuric acid [16]. The produced palladium sulfide (Pd₄S) catalysts deposited on carbon nanofibers exhibited the mono-hydrogenation activity in the gas-phase butadiene reduction producing butenes of various forms in good yields (99% of butenes at 100% conversion: the selectivities among various butenes are not reported). In contrast to Pd metal-based catalysts, this Pd₄S catalyst presented high stability under reaction conditions while having significant activity and appropriate selectivity for partial hydrogenation of dienes.

Thiolate self-assembled monolayers deposited on Pd/Al₂O₃ catalysts could also direct the catalytic activity of heterogeneous systems for fatty acid diene hydrogenation as shown in **Figure 4** [17]. In comparison, the uncoated Pd/Al₂O₃ catalyst produced the fully hydrogenated fatty acids under the same hydrogenation condition. This selectivity is attributed to steric effects between thiolate monolayers and

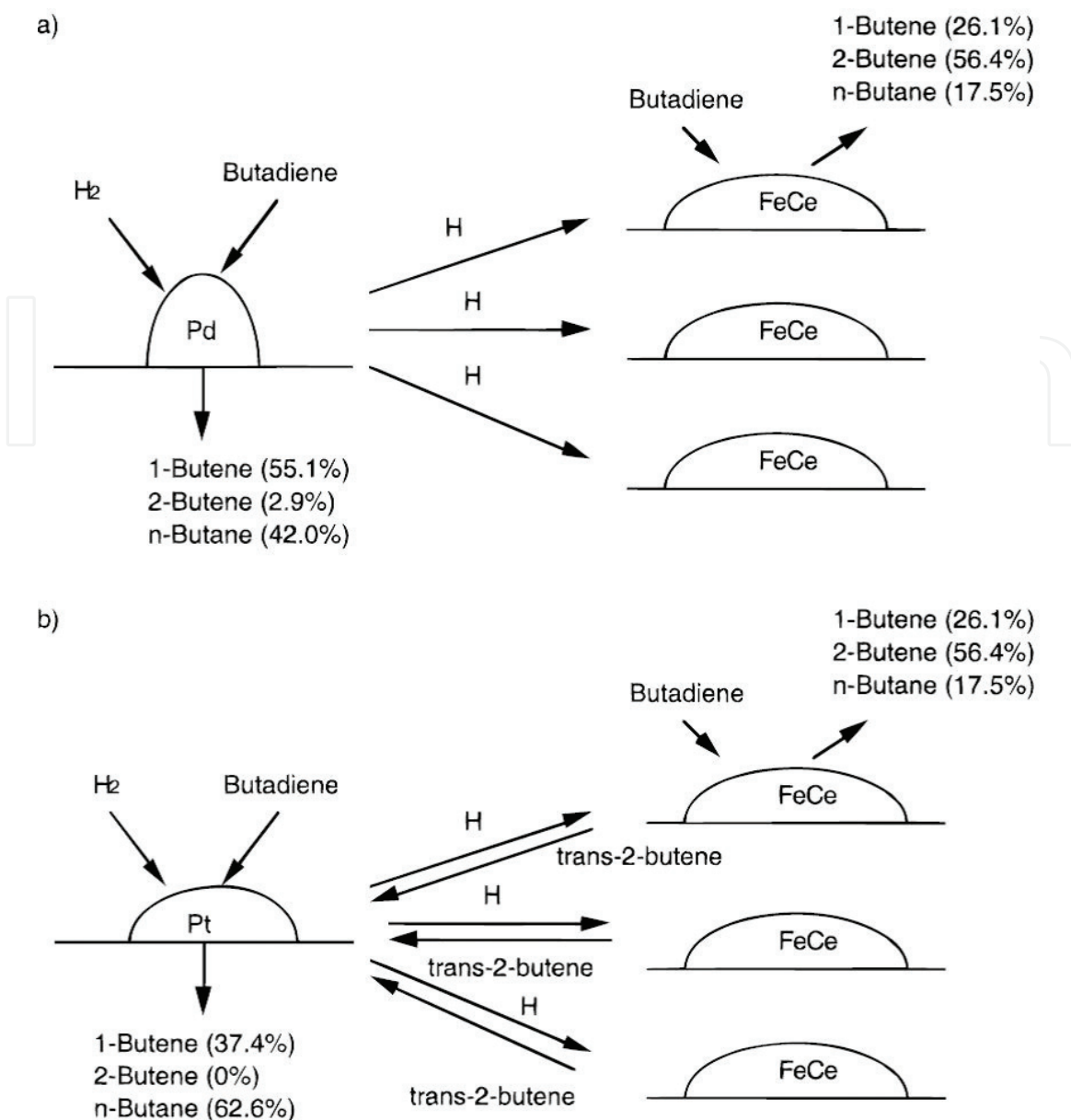


Figure 3. The working hypothesis of physical mixtures for 1,3-butadiene hydroisomerization. (a) Pd containing mixtures and (b) Pt containing mixtures. Reproduced from [13] with permission from the American Chemical Society.

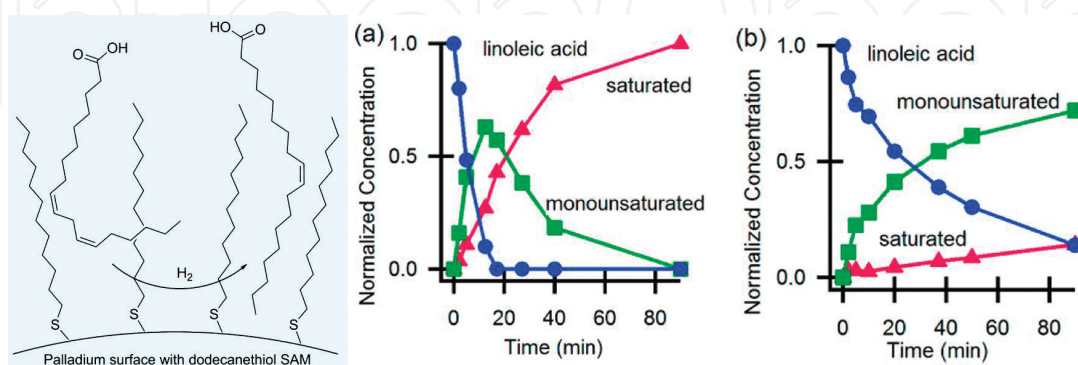


Figure 4. Kinetic data for linoleic acid hydrogenation over Pd/Al₂O₃ at 30°C and 6 bar H₂. (a) Uncoated Pd/Al₂O₃ and (b) dodecanethiol-coated Pd/Al₂O₃. Reproduced from [17] with permission from the American Chemical Society.

fatty acid reactants based on the kinetic studies and ligand chain length studies reported in this work. The influence of ligand chemical functionality was also investigated in this study. The results showed that unlike hydrophobic

alkanethiolate ligand modifiers, the hydrophilic thioglycerol modifiers strongly inhibited the catalytic activity of Pd/Al₂O₃ surfaces.

2.2.2 Supported metal nanoparticle catalysts: the nano effects

More and more researchers consider nanoparticles as a better option for catalytic reactions due to their high surface area per volume characteristics. In the area of heterogeneous catalysis, the complete analyses of catalyst sizes, compositions, and distributions are now required and many well-known active solid-state catalysts including carbon-supported Pd are found to be actually in nanoscale. With the advancement of nanomaterials synthesis and characterization, the nanoscale catalysts are now designed and prepared to tune their activities for desired applications including diene hydrogenation. For example, Pd nanoparticles stabilized with dendrimers (polypropylenimine, PPI) deposited on a silica surface are used for catalysis application (**Figure 5**) [18]. The internal amine functional groups on PPI dendrimers are used as a ligand to encapsulate Pd nanoparticles and the external amine groups help grafting the dendrimers on a polyamine-modified silica surface to form the immobilized dendrimer catalyst composite. The dendrimers around the under-deposited nanoparticle increase the selectivity of the Pd nanoparticles and decrease the Pd metal leaching. The immobilized dendrimer catalyst reveals higher reactivity for the selective hydrogenation of dienes than the traditional heterogeneous catalysts. In this study, Karakhanov et al. further discussed the effects of size and substituent pattern of the substrate, 2,5-dimethyl-2,4-hexadiene, during the catalytic hydrogenation (**Table 3**). Since both C=C double bonds in 2,5-dimethyl-2,4-hexadiene are internal and highly substituted at C2 and C5 positions, the rate of the reaction is relatively slow but the overall reactions result in the high yield of thermodynamic 1,4-addition product.

Instead of using modifier or poisoning agents to change the catalytic activity of heterogeneous metal substrates, the modification of support materials to induce the steric-related selectivity has been successfully attempted [19]. By overcoating Pd nanoparticle catalyst with porous alumina using atomic layer deposition, Yi et al. could produce a highly stable (against deactivation) and selectivity for mono-hydrogenation of 1,3-butadiene to butenes (**Figure 6**). The selective hydrogenation worked well even in the presence of excess propene. The alumina overcoat clearly suppressed the conversion of propene to propane very efficiently while maintaining ~100% butenes selectivity with ~100% 1,3-butadiene conversion. This is attributed

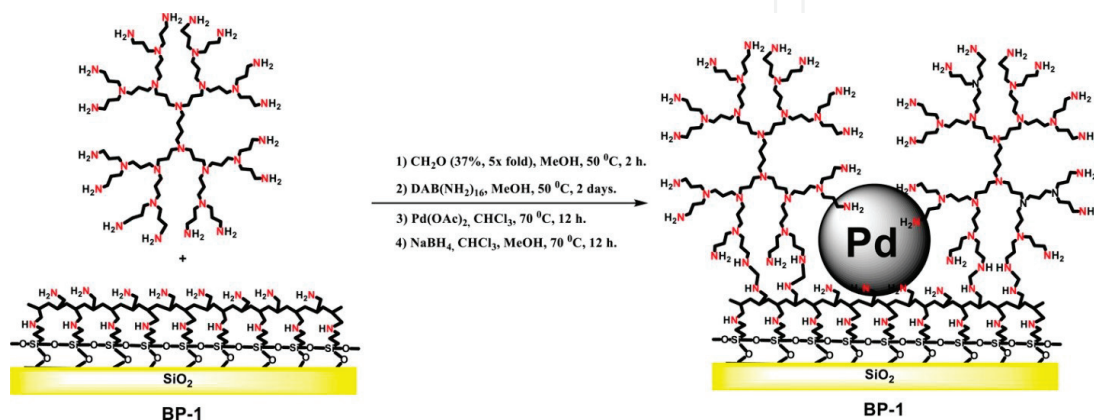
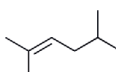
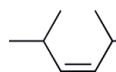
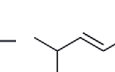
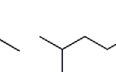


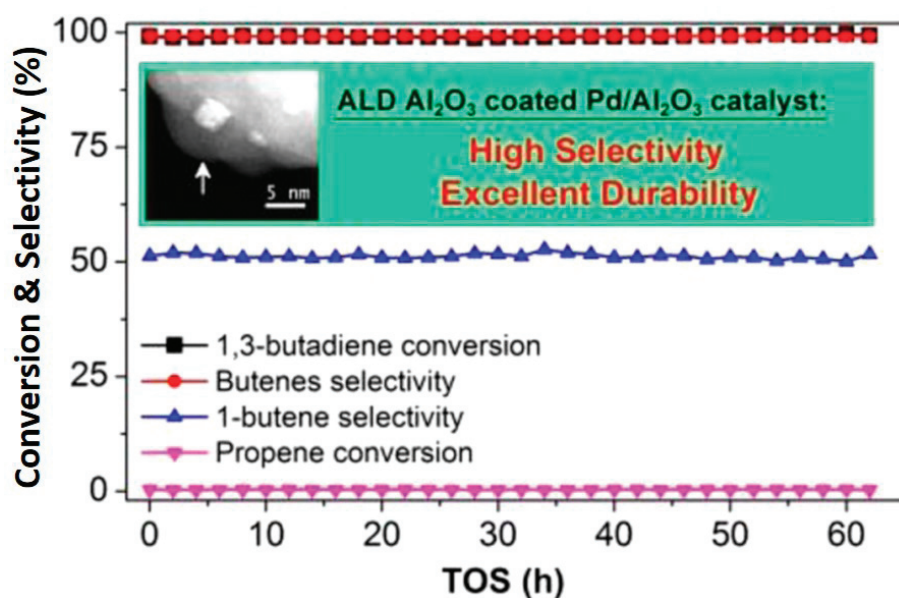
Figure 5. Polypropylenimine (PPI)-modified palladium nanoparticle catalyst composite. Reproduced from [18] with permission from the American Chemical Society.

Entry					Product distribution			
	P, MPa	t, h	Sub/Pd	Conv.,%				
1	1	1	3680	100	16.5	22	58	4
2	3	1	3680	100	17.5	23.5	53	5
3	1	0.25	3680	100	20	26	51	4.5
4	1	0.25	7360	91.5	9	64.5	25.5	1

Data reproduced from [18].

Table 3.

The catalytic reactions of 2,5-dimethyl-2,4-hexadiene with Pd nanoparticle composite in 2 mL toluene at 70°C and under 3 MPa H₂.

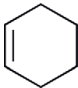
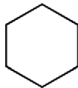
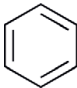
**Figure 6.**

Catalytic property of microporous alumina-coated Pd/Al₂O₃ using atomic layer deposition (ALD) for 1,3-butadiene hydrogenation in the presence of an excess propene. Reproduced from [19] with permission from the American Chemical Society.

to the confinement effect within the micropores of the alumina overcoat and the stronger adsorption of 1,3-butadiene than alkenes on Pd nanoparticle catalysts.

Mesoporous carbon films as support to control the activity of Pd catalyst also reported for the selective hydrogenation of 1,3-butadiene [20]. The material synthesis involves the co-deposition of small polymeric carbon clusters, structure filling agents, and Pd ions on a substrate (**Scheme 1**). Thermal treatments converted these hybrids into graphitized microporous carbon with active Pd catalysts. These catalysts were highly active in the gas-phase mono-hydrogenation of 1,3-butadiene to butenes. The major product for these catalytic systems is 1-butene at ~50% selectivity among butene isomers, which is very similar to the catalytic selectivity of porous alumina-coated Pd catalysts described above.

Bimetallic Au-Pd alloy catalysts with low amount of Pd were prepared by either co-deposition-precipitation or co-impregnation procedure [21]. This approach is especially beneficial considering the low usage of somewhat toxic Pd metals. These bimetallic catalysts could selectively hydrogenate 1,3-butadiene in the presence of propene. By changing the Au/Pd ratio, the catalytic activity of bimetallic catalysts could be further controlled. The overall selectivity among butene isomers also depended on the reaction temperatures. At the lower temperature, 1-butene was

Entry	Catalyst	Time (h)	Conv. (%)	 (%)	 (%)	 (%)
1	G0, C1	1.75	>99	76	24	—
2	G1-C2, C2	0.5	21	>99	—	—
3		20	>99	88	10	2
4	G1-C6, C3	0.5	11	>99	—	0
5		20	72	97	1.5	1.5
6	G1-C12, C4	0.5	15	>99	—	—
7		20	20	>99	—	—
8	G2-C6, C5	0.5	N.R.	—	—	—
9		20	>99	73	11	6
10	G2-C12, C6	0.5	24	>99	—	—
11		5	>99	80	14	6

GC and NMR are used to monitor the reaction.
Data reproduced from [22].

Table 4.

Hydrogenation of 1,3-cyclohexadiene with silica supported PAMAM-palladium complex catalyst (5.25 mmol 1,3-hexadiene, 10 μ mol Pd catalyst complex, 5 mL methanol, pressurized glass autoclave to 14 psi H_2 , 25 $^{\circ}$ C).

the catalysis results shown in Entries 3, 5, and 7 indicate the increased conversion of reactants with the formation of some minor full hydrogenation products. The results suggest that the primary product, cyclohexene, would compete with the diene reactant for the catalytic active sites. When the concentration of 1,3-cyclohexadiene is high at the beginning of the reaction, diene would dominate the adsorption on the active sites and the reaction would maintain a good selectivity to cyclohexene. With the increased concentration of cyclohexene at the later stage of the reaction, the adsorption on active catalytic sites starts to take place. The reactions are generally slower for G1 catalysts compared to G0 catalyst especially with longer linkers. The G2-C12 catalyst, however, exhibits good activity and selectivity toward cyclohexene indicating the importance of right combination between dendrimer generations and linker lengths. A trace amount of benzene was also observed for some of the catalysts. The catalytic reactions of other acyclic dienes also are investigated to understand the effects of substrate structure. In general, the 1,2-addition hydrogenation of less hindered C=C is the most favorable compared to that of more hindered C=C, 1,4-addition hydrogenation, and full hydrogenation.

Zeolite- and magnesium oxide-supported molecular rhodium complexes are also tested for the hydrogenation of 1,3-butadiene [23]. The selectivity for mono-hydrogenation increases when the Rh species nucleation decreased from several atoms to dimeric clusters. The poisoning with CO ligands further increases the mono-hydrogenation selectivity, especially when electron donating MgO is used as a support (>99% selectivity for mono-hydrogenation as shown in **Figure 8**). This is attributed to limiting the activity for H_2 dissociation and preventing the additional hydrogenation to butane.

2.3 Metal complexes and supported materials for the hydrogenation of trienes

Selective hydrogenation of triene is also an important topic for fine chemicals and pharmaceutical industries [3]. Myrcene with one isolated C=C bond and two

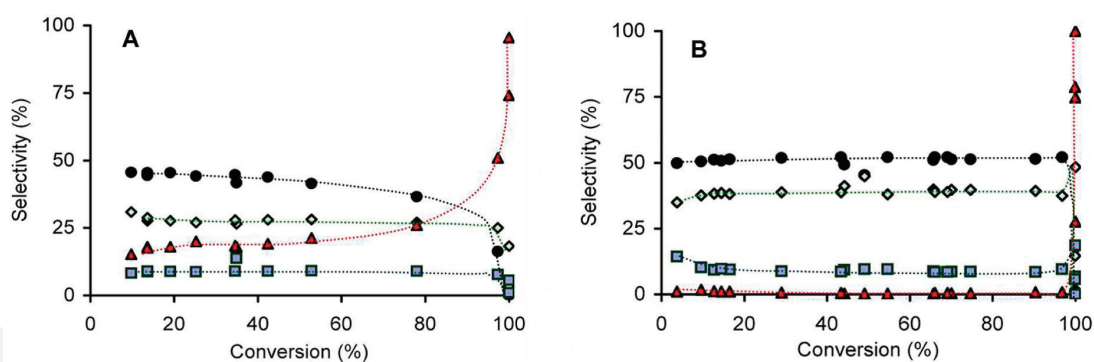


Figure 8. Selectivity plots for MgO-supported rhodium dimers in the absence (A) and in the presence (B) of CO ligands in the hydrogenation of 1,3-butadiene (filled circle: 1-butene, open diamond: trans-2-butene, blue square: cis-2-butene, red triangle: butane). (Reactions condition: 2 vol % 1,3-butadiene, balanced with H₂, total pressure = 1 bar, room temp) Reproduced from [23] with permission from the American Chemical Society.

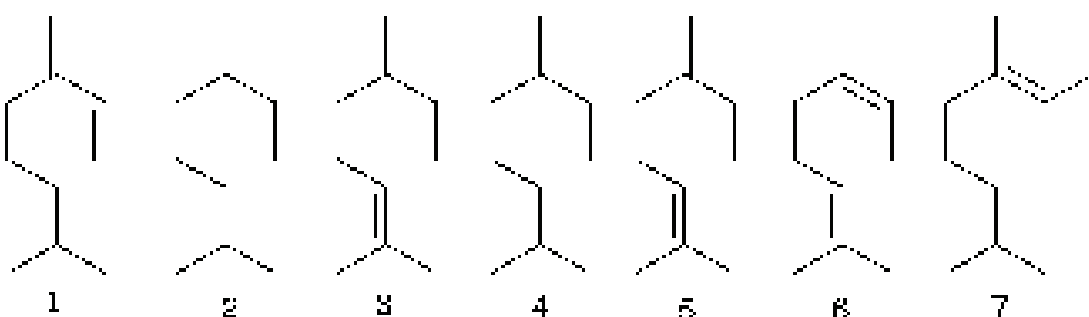


Figure 9. Reactant (1) and potential products (2–7) for myrcene hydrogenation. Products 4–7 are dienes. Reproduced from [24] with permission from the Sciencedirect.

conjugated C=C bonds can be synthesized by the pyrolysis of β -pinene in nature. Despite the availability of myrcene, only little success in selective hydrogenation of the substrate to diene have been made. Gusevskaya et al. reported the hydrogenation of myrcene either by using metal complex ion or heterogeneous sol-gel catalysts [24, 25]. For 10% palladium on carbon (Pd/C) under 20 atm of H₂ and cyclohexane solvent system at 80°C, full hydrogenation reaction would take place within 30 min, and the catalytic system does not have any selectivity toward diene or monoene. On the other hand, the transition metal complexes of [RuCl₂(CO)₂(PPh₃)₂], [RhH(CO)(PPh₃)₃], [IrCl(CO)(PPh₃)₂], and [Cr(CO)₆] show the capability to form diene products in relatively good yields (**Figure 9** and **Table 5**) [24].

From Entries 1–4 in **Table 5**, the reactivity of the metal complexes under the same condition turns out to be Ru < Cr < Ir < Rh. Ru and Rh complexes show slightly higher selectivity toward monohydrogenated products, dienes, than chromium and iridium complexes. Rh complex is further tested by adding extra PPh₃ ligand in the reaction (Entry 5). The presence of extra PPh₃ slows the reaction down requiring higher reaction temperature, but increases selectivity toward dienes. The similar selectivity of myrcene hydrogenation is achieved by simply changing solvent from cyclohexane to benzene even at the lower reaction temperature of 80°C. The reaction only produces a trace amount of double or full hydrogenation products. However, the selectivity among different dienes (Entries 4–7) is still poor.

The first hydrogenation of myrcene, a triene, takes place at the conjugated diene group instead of the isolated and hindered alkene group. The 1,2-addition of conjugated diene produces either compound 4 or compound 5. The 1,4-addition of conjugated diene involving Pd-allyl intermediates produce compounds 6 and 7, the

Run	Catalyst	Time (min) ^a	T (°C)	S (%) ^b	Product distribution (%)					
					2	3	4	5	6	7
1	[RuCl ₂ (CO) ₂ (PPh ₃) ₂]	110	100	83	1	16	7	32	9	35
2	[Cr(CO) ₆]	45	100	74	4	22	8	26	29	11
3	[IrCl(CO)(PPh ₃) ₂]	15	100	76	4	20	8	22	33	13
4	[RhH(CO)(PPh ₃) ₃]	5	100	87	4	9	13	24	34	16
5	[RhH(CO)(PPh ₃) ₃] ^c	24	140	96	tr.	4	14	31	26	25
6	[RhH(CO)(PPh ₃) ₃] ^d	60	80	98	tr.	2	15	27	34	22

^aReaction time necessary for ca. 80% conversion.
^bSelectivity for monohydrogenated products 4–7 at ca. 80% conversion.
^cPPh₃ was added (0.17 mmol).
^dBenzene was used as a solvent.
 Data reproduced from Ref [24].

Table 5.

The catalytic reaction of metal ion catalyst with myrcene, compound 1, under 20 atm H₂ and cyclohexane solvent.

E-Z isomers. Based on the results in **Table 5**, the major diene products are compound 5 and 6. This is due to the higher reactivity of terminal alkene in myrcene, which undergoes the coordination of the primary alkene group followed by the hydrogen addition. These isolated diene products 4–7 are further hydrogenated to monoene 3 with the addition of hydrogen to less sterically hindered alkene. When the reaction is continued, the yield for full hydrogenation product 2 constantly increases. Since there are several pathways for the hydrogenation of myrcene and the reactions generate many different mono- and di-hydrogenation products, this reaction is extremely difficult to control and hard to predict with regarding the overall selectivity. However, there are some correlations between the yields of products and the kinetics/thermodynamics of intermediates and products. For example, the kinetic reactivity among diene products should follow the ensuing order: 4 > 5 > 6 > 7.

For the hydrogenation of myrcene by sol-gel Pd/SiO₂ catalyst, the selectivity for dienes is higher than that of the metal complex catalyst [25]. Robles-Dutenhefner et al. used three different temperatures for the reactions, the catalysis results show

Run	Catalyst (wt. %)	T (°C)	Time (min)	Conv. (%)	S (%) ^a	Product distribution (%)				
						2	3	4	5	6 + 7
1	1% Pd/SiO ₂ /300°C (0.5)	80	15	100	0	100				
4	1% Pd/SiO ₂ /1100°C (0.5)	80	15	75	100			20	18	62
			60	96	94	1	5	16	16	62
5	1% Pd/SiO ₂ /1100°C (0.5)	100	15	80	99		1	18	15	66
6	1% Pd/SiO ₂ /1100°C (2.5)	80	15	75	98	1	1	18	15	65
8	3% Pd/SiO ₂ /1100°C (0.5)	80	60	96	97	1	2	20	15	62

^aSelectivity for monohydrogenated products 4–7.
 Data reproduced from Ref [25].

Table 6.

Hydrogenation of myrcene catalyzed by Pd/SiO₂ in cyclohexane under 20 atm H₂.

that the reaction temperature would greatly affect the reactivity of the Pd/SiO₂ catalysts. BET surface area analysis shows the change in synthesis temperature that would cause some variations in the pore size of the catalyst. Since the pore is created by the presence of organic solvent during the synthesis process, the high temperature at or above 300 °C would generate the largest pore size due to increased gas pressure. However, unstable gaseous environment at higher temperature of 1100 °C causes the collapse in its pore resulting in the decreased surface area and pore size.

The catalysis results for myrcene hydrogenation in **Table 6** show that the selectivity toward dienes by mono-hydrogenation is higher than 90%. The Pd/SiO₂ catalyst with a larger pore created at 300 °C converts the reactant to saturated organic compound without forming any alkene. Due to the higher surface energy of this catalyst with a large pore, the substrates are readily adsorbed on the catalyst surface and undergo full hydrogenation. For the Pd/SiO₂ heated at 1100 °C, the lower surface energy of the catalyst makes the activity to be decreased. The hydrogenation of isolated alkene would become unfavorable and the high selectivity to form dienes from myrcene is observed for this Pd/SiO₂ heated at 1100 °C. The ratio of the E/Z isomer (compound 6 and 7) is 0.176.

3. Semi-heterogeneous nanoscale catalysts

3.1 Semi-heterogeneous colloidal nanoparticles in ionic liquids

Colloidal nanoparticle catalysts are considered semi-heterogeneous due to their homogeneous characteristics (kinetic efficiency) accompanied by their heterogeneous surface property. Semi-heterogeneous catalyst can be benefited from the advantages that both homogeneous and heterogeneous catalysts have. Nanoparticle catalysts can have a higher catalytic activity than their bulk and heterogeneous counterparts, especially with nano-effects of high surface area to volume ratio. They can also be easily separated from the products and recycled similar to other heterogeneous catalytic systems.

Semi-heterogeneous nanoparticle catalysts used for the hydrogenation of dienes show the relatively good selectivity and reactivity even compared to the traditional homogeneous catalysts. Ionic liquid-stabilized Pd nanoparticle catalyst shown in **Figure 10** is one of those examples used for diene hydrogenation [26]. The thin film of ionic liquid with the hydrophobic anion PF₆⁻ on the Pd nanoparticle surface (Pd/sgPF₆) enhances the solubility in methylene chloride and the selectivity of the catalyst. The ionic liquid on the surface acts like a cage to control which substrate would pass through the liquid ion film and reach the particle surface for catalytic reaction. The liquid ion film on catalyst creates the non-equilibrium environment, so that the rate determining step could easily be observed.

Several conjugated and isolated diene compounds are tested for the catalytic hydrogenation using Pd/sgPF₆, the hydrophobic ionic liquid nanoparticle catalyst (**Table 7**). The results show that the conjugated cyclodienes (Entries 1 and 3) are much more reactive than the isolated cyclodienes (Entries 2 and 4). The catalytic reactions of cyclohexa-1,3-diene **8** and cycloocta-1,3-diene **13** produce mono-hydrogenation products almost quantitatively. Once the monoene is formed, the further hydrogenation does not take place due to the weaker adsorption of monoenes on Pd nanoparticle surface. The adsorption of dienes on Pd nanoparticle surface by two π bonds coordination is much more preferred because Pd atom is electron deficient. In addition, the mono-hydrogenation products have lower

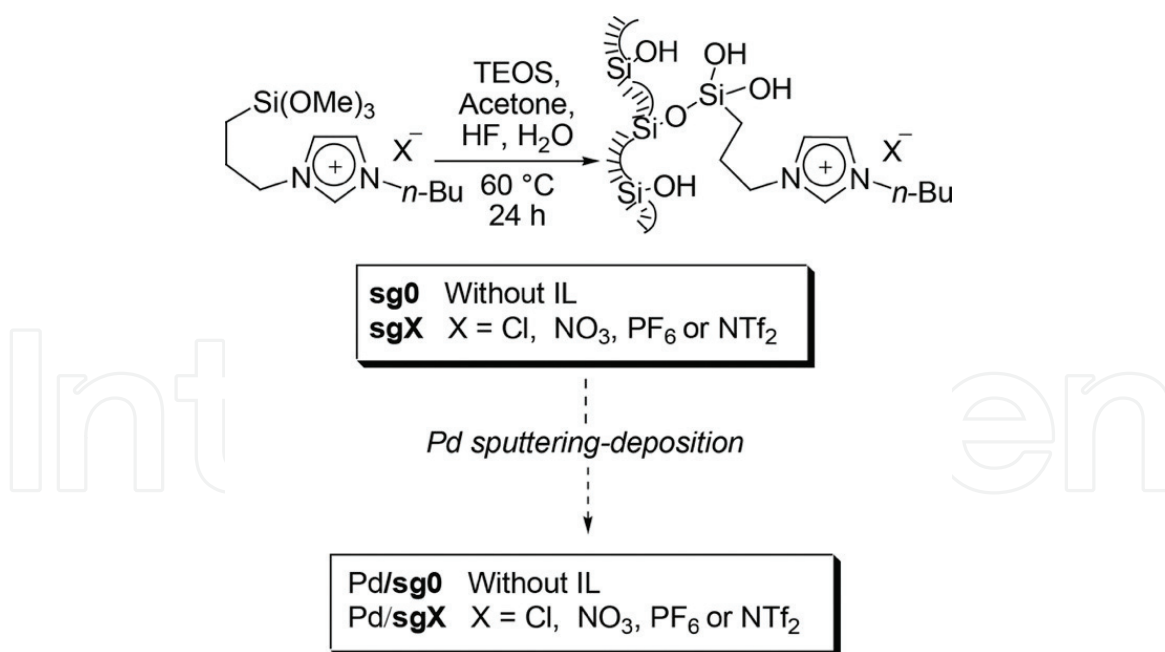


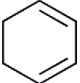
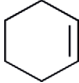
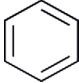
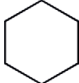
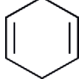
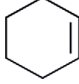
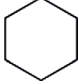
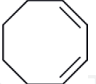



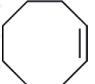

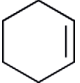
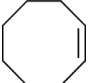
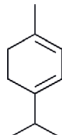
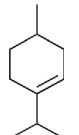
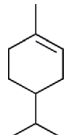
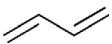
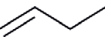
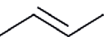

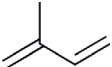
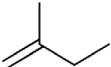
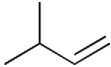
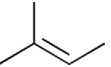
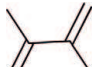
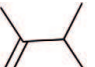
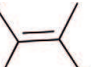
Figure 10.

Synthesis of ionic liquid hybrid palladium nanoparticle by sputtering-deposition. Reproduced from [26] with permission from the American Chemical Society.

solubility in ionic liquid than diene reactants, which readily transfer through the liquid ion film. This makes monoene to be evicted out from the ionic liquid inhibiting the second hydrogenation. For isolated cyclohexa-1,4-diene **12** and cycloocta-1,5-diene **16**, the reactivity and selectivity to generate monoene are similar, but the overall conversion yields are extremely low. The low reactivity of monoene compounds is confirmed from the catalytic reactions of cyclohexene (Entry 5) and cyclooctene (Entry 6). Both substrates are unreactive for hydrogenation condition. The reaction of unsymmetrical cyclohexa-1,3-diene **17** (Entry 7) results in high conversion yields for mono-hydrogenation products with a preference for the hydrogenation of less hindered alkene group. Due to the steric hindrance of methyl and isopropyl groups, the 1,4-hydrogenation product is not formed. For the larger-conjugated dienes, the catalytic reactivity decreases with increased steric hindrance of alkyl substituent groups (Entries 9–11). However, the opposite trend for selectivity toward internal alkene is observed. As the number of alkyl substituents around C=C bonds increases, the yield for thermodynamic 1,4-hydrogenation product also increases. Moreover, the deuterium gas studies also show the actual mechanism for the cyclohexa-1,3-diene hydrogenation by ionic liquid catalyst. The conversion from cyclohexa-1,3-diene to cyclohexene is mainly through the 1,2-hydrogenation reaction with 92% selectivity and the ratio of 1,2-addition/1,4-addition around 1.7.

3.2 Semi-heterogeneous dendrimer-encapsulated metal nanoparticles

The catalytic property of polypropylenimine (PPI)-Pd nanoparticle hybrids is examined by the hydrogenation of isoprene substrate (**Table 8**) [27]. The reaction generates 2-methyl-2-butene (1,4-addition product) as the major product and 3-methyl-1-butene and 2-methyl-1-butene (1,2-addition products) as the minor products. The selectivity of the catalytic reaction is dependent upon the pressure of applied hydrogen gas and the ratio of substrate and catalyst. Higher hydrogen pressure and low substrate/catalyst ratio would result in decreased selectivity for monohydrogenation product. PPI dendrimer would enhance the catalytic selectivity to form monoene because it would limit the adsorption of the primary monoene

Entry	Diene	TOF (Conv.) ^a	Products (Selectivity/%)		
1	 8	3.0 (>99)	 9 (97)	 10 (2)	 11 (1)
2	 12	0.1 (<2)	 9 (>99)	 11 (<1)	
3	 13	13.0 (>99)	 14 (>99)	 15 (<1)	
4	 16	0.3 (<4)	 14 (>99)	 15 (<1)	
5	 9	— (<1)	—		
6	 14	— (<1)	—		
7	 17	6.2 (>99)	 18 (67)	 19 (33)	
9	 20	11.6 (>99)	 21 (36)	 22 (54)	 23 (10)
10	 24	3.7 (>99)	 25 (18)	 26 (7)	 27 (75)
11	 28	0.7 (>99)	 29 (19)	 30 (81)	

Conversion determined by GC.

^aTOF = mol substrate converted/(mol Pd surface • s).

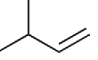
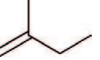
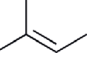
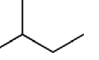
Data reproduced from [26].

Table 7.

Selective hydrogenation of dienes by Pd/sgPF₆ catalyst under optimized conditions (Reaction condition: Pd/sgPF₆ catalyst (0.1 μmol Pd), substrate/Pd = 5000, 10 mL of CH₂Cl₂, 4 bar H₂, 40 °C and 250 rpm).

product on the Pd surface and minimize the further hydrogenation to 2-methylbutane.

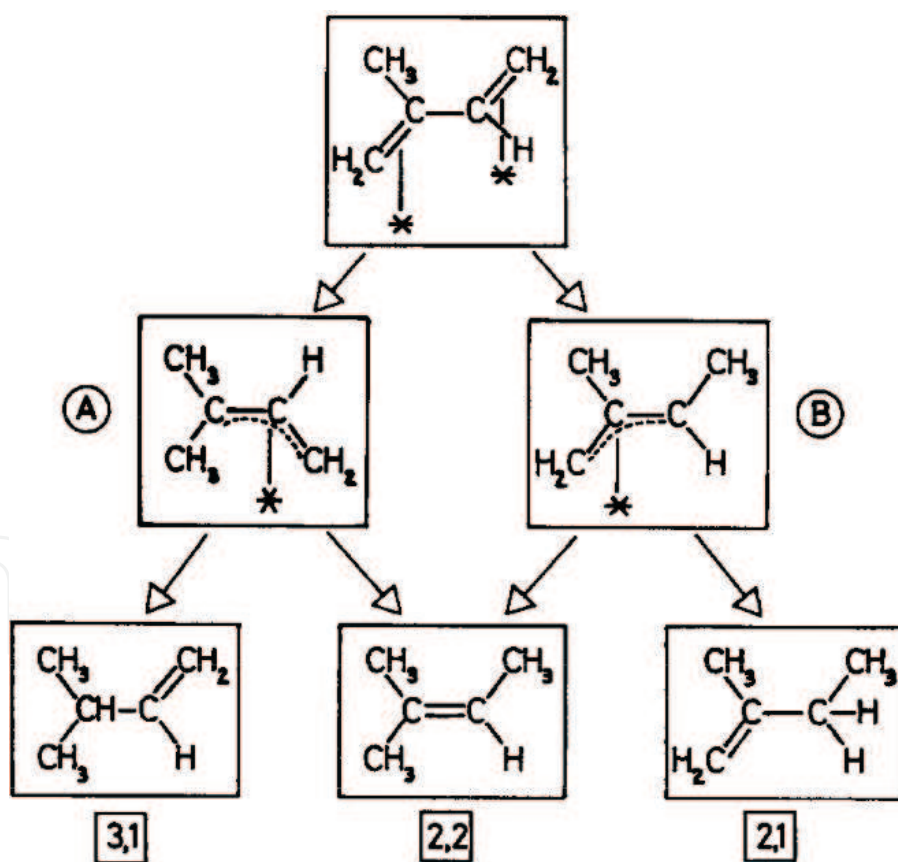
Other possible reasons for the high selectivity toward 1,4-addition product are also proposed. First, the initially produced 1,2-addition products could be isomerized to 1,4-addition product due to the higher stability of 2-methyl-2-butene. Second, the methyl group on isoprene would affect the stability of π-allyl intermediate (**Figure 11**) [6]. The intermediate A would generate two different products, 3-methyl-1-butene or 2-methyl-2-butene. In regards to the steric effect of intermediate A at C2 and C4, C4 has less substituted groups around C=C compared to C2. Therefore, it is easier for the second hydrogen to add on C4, and increase the yield of 2-methyl-2-butene. For the intermediate B, it is also easier for hydrogen atom to transfer to C1 since C3 is relatively more hindered than C1, which results mostly in 2-methyl-2-butene. The steric hindrance also directly influences the relative yield of 3-methyl-1-butene (higher) compared to that of 2-methyl-1-butene (lower).

Entry	P, MPa	t, h	Sub/Pd ^a	Conv., %	Selec. on alkene, %	Product distribution			
									
1	1	1	3680	100	96	16.5	22	58	4
2	3	1	3680	100	95	17.5	23.5	53	5
3	1	0.25	3680	100	95.5	20	26	51	4.5
4	1	0.25	7360	91.5	99	9	64.5	25.5	1
5	3	0.25	7360	100	91	16.5	24	50.5	9
6	3	0.25	14,720	100	93.5	20.5	25	48	6.5
7	3	0.25	22,080	100	94	22	24.5	47.5	6
8	3	0.25	66,240	83	98.5	19	30	49	2

^aMol/mol ratio.
Data reproduced from [27].

Table 8.

The catalytic reactions of isoprene with Pd nanoparticle composite in 2 mL toluene at 70°C and under 3 MPa H₂.

**Figure 11.**

Reduction pathway for isoprene to form monoene product. Reproduced from [6] with permission from the American Chemical Society.

Ornelas et al. also studied the semi-heterogeneous catalysis by using dendrimer-passivated palladium nanoparticle as a catalyst for the hydrogenation of dienes [28]. They synthesized the 1,2,3-triazole heterocycles-capped palladium nanoparticle catalyst that exhibits the higher reactivity to diene hydrogenation compared to the

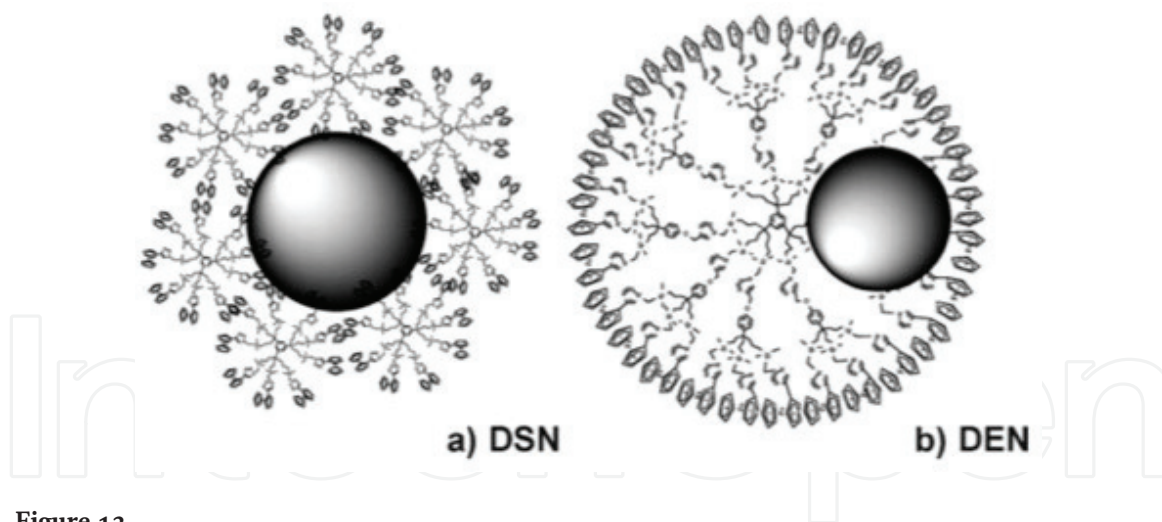


Figure 12.

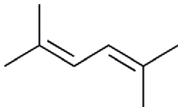
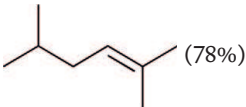
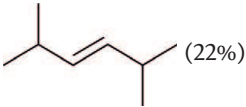
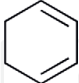
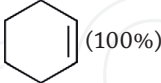
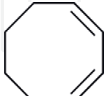
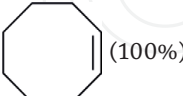
(a) Generation 1, dsn, and (b) generation 1, den, Pd nanoparticle encapsulated by PAMAM. Reproduced from [28] with permission from the Royal Society of Chemistry.

PAMAM dendrimer-encapsulated Pd nanoparticle catalyst. Depending on the generation of the triazole dendrimer, the catalyst could develop into different morphologies that control the activity and selectivity. When the G_0 dendrimers are used, the interdendrimer-stabilized palladium nanoparticle (DSN) is formed (**Figure 12**). For the higher generation dendrimers, the intradendrimer-encapsulated palladium nanoparticle (DEN) is produced. Due to the smaller size of the G_0 dendrimer, the Pd nanoparticle cannot be encapsulated by dendrimer and needs to be stabilized by several G_0 dendrimer. This makes the overall size of DSN relatively larger than the other higher generation dendrimer-capped catalysts.

When the higher generation dendrimer is used, the large size of dendrimer allows enough Pd ions to be encapsulated in the interior of dendrimer and the following reduction generates dendrimer-encapsulated Pd nanoparticles. Unlike PAMAM-stabilized metal nanoparticle, 1,2,3-triazoleferrocenyl dendrimer-stabilized Pd nanoparticle would have higher stability during the catalyst reaction [28]. The nature of the reducing agent and the generation of dendrimer are found to have noticeable influence on the reactivity and stability of each catalyst. DEN- G_1 reduced by methanol has the best reactivity for the mono-hydrogenation of diene, which indicates that the smaller size of the Pd nanoparticle increases the reactivity. Moreover, the unique structure of 1,2,3-triazoleferrocenyl dendrimer is also found to be the another reason for catalyst to have higher reactivity. **Table 9** shows DEN- G_1 has higher reactivity to small dienes for mono-hydrogenation. However, the catalytic reactions of large dienes with steric bulkiness are slightly slower. Hydrogenation of trienes mostly results in the formation of monoene compounds indicating the high activity of diene intermediate after mono-hydrogenation. More substituted dienes tend to have a lower catalytic reactivity. Moreover, the isomerization of terminal monoenes and the trace amount of the 1,4-hydrogenation product from highly substituted dienes are also observed in the reaction.

3.3 Well-defined small organic ligand-capped palladium nanoparticles as semi-heterogeneous catalysts

Many ligand-passivated nanoparticles have been used as semi-heterogeneous catalysts. Since the surface ligands that stabilize nanoparticles from aggregation can have either hydrophobic or hydrophilic property, they can be soluble in various solvents including organic and aqueous solutions. Shon group has developed the thiosulfate protocol using alkanethiosulfate as a ligand precursor to passivate and

Substrate	Product (yield)	TOF ^a
	 (78%)	810
	 (22%)	230
	 (100%)	1150
	 (100%)	530

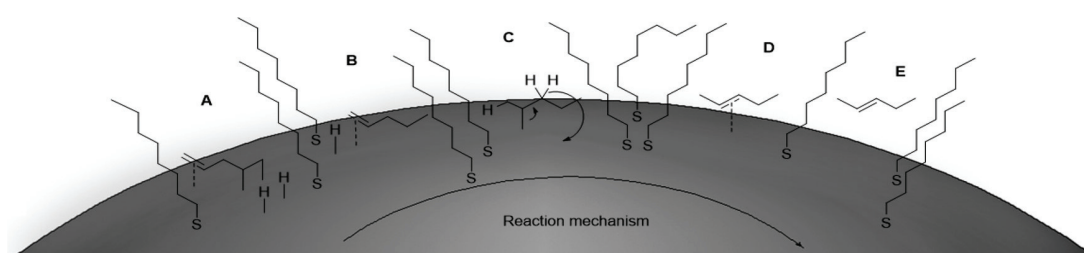
^aTOF were determined by the yield of formation and final product.
Data reproduced from [28].

Table 9.

Hydrogenation of olefins catalyzed by methanol reduced DEN-G₁ (Reaction condition: 25 °C, 1 atm H₂, and substrate/Pd ratio is 1000 in mixed solvent CHCl₃/MeOH = 2).

stabilize the catalytically active palladium nanoparticle surface [29–33]. The hydrophobic alkanethiolate ligand gives the nanoparticle high solubility in nonpolar organic solvent. Since alkanethiosulfate offers slower passivation activity, the surface ligand density of alkanethiolate on Pd nanoparticles can be controlled. Therefore, the alkanethiolate-capped Pd nanoparticles generated from alkylthiosulfate exhibit good catalytic activity and selectivity toward various organic reactions including isomerization and hydrogenation. Hexanethiolate- and dodecanethiolate-capped Pd nanoparticles show unique catalytic properties for the reaction of allyl alcohol under the atmospheric pressure of hydrogen gas at room temperature [30, 31]. Allyl alcohol can undergo either hydrogenation to 1-propanol or isomerization to propanal.

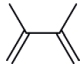
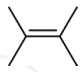
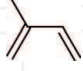
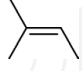
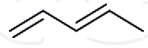

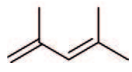
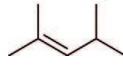
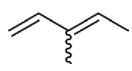
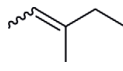
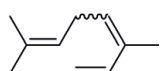
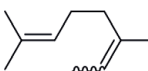
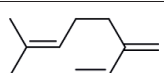
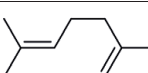
Octanethiolate-capped Pd nanoparticle (C8 PdNP) with average core size of ~2.3 nm is synthesized and its composition and structure are confirmed by various instruments. Alkanethiolate-capped Pd nanoparticles are investigated for the catalytic reaction of 1,4-pentadiene [32]. The mechanistic studies show that mono-hydrogenation of isolated dienes would take place on one of the terminal C=C bond (**Figure 13**). The di- σ -bonded Pd intermediate **A** would form after the di- π -bond adsorption on Pd, which leads to the mono-hydrogenation and the formation of 1-pentene. The further isomerization via mono- σ -bonded Pd intermediate converts 1-pentene to the isomerized product, 2-pentene.

**Figure 13.**

The proposed mechanism (from A to E) for 1,4-pentadiene catalytic reaction under H₂ environment. Reproduced from [32] with permission from the Royal Society of Chemistry.

The C8 PdNP is used as the catalyst for the hydrogenation of various conjugated diene and triene substrates as shown in **Table 10** [33]. The catalytic reactions of conjugated dienes with different substitution patterns around C=C bonds produce almost exclusively the mono-hydrogenation products (**Table 10**, Entries 1–5). In addition, the hydrogenation of trienes (Entries 6 and 7) also results in the high yields of isolated dienes, the mono-hydrogenation products. This reactivity confirms the important role of alkanethiolate ligands on controlling the activity of Pd catalyst surface. With its surface passivated by organic ligands, nanoparticle could maintain a good stability, so that it could avoid aggregation and keep the large surface area intact. The surface ligand could block the more active site (terrace surface) for hydrogenation and promotes selective hydrogenation of dienes. The analysis of final monoene compositions showed that the major product is the 1,4-addition product and the minor product is the 1,2-addition product. The kinetic study of diene to monoene proved that the high selectivity for the 1,4-addition product is the result of both initial 1,4-addition reaction and the subsequent isomerization of terminal alkene, the 1,2-addition product, into internal alkene.

After the first hour of reaction, the conversion of diene in entry 1 reaches over 50% with the ratio of 1,4-/1,2-addition products at 3.43. The consumption of reactant is almost complete after 5 h reaction with the ratio of 1,4-/1,2-addition products at 4.90. The yield of the 1,4-addition product is continuously increasing after 5 h reaction with the ratio of 1,4-/1,2-addition products increasing to 10.30 at the 24 h reaction. This clearly indicated that the isomerization of the terminal alkene to the internal alkene is the reason for the high selectivity of 1,4-addition product. The selectivity between the 1,4- and 1,2-addition products are also summarized for other diene and triene substrates as shown in **Table 10**. C8 PdNP clearly showed high selectivity for the 1,4-addition product, the thermodynamically more stable product. C8 PdNP clearly exhibits excellent selectivity to form internal alkene, the mono-hydrogenation and 1,4-addition product, compared to other reported catalytic systems. Not only the conversion yields and selectivity are superior but also the reaction condition (room temperature and atmospheric pressure) is much

Entry	Substrate	Reaction condition	Major product (%)
1		C8 PdNP 24 h	 (91% 1,4-) + (9% 1,2-)
2		C8 PdNP 24 h	 (93% 1,4-) + (7% 1,2-)
3		C8 PdNP 24 h	 (92% 1,4-) + (8% 1,2-)
4		C8 PdNP 24 h	 (90% 1,4-) + (7% 1,2-)
5		C8 PdNP 24 h	 (90% 1,4-) + (5% 1,2-)
6		C8 PdNP 24 h	 (59% 1,4-) + (41% 1,2-)
7		C8 PdNP 24 h	 (69% 1,4-) + (23% 1,2-)

Data reproduced from [29].

Table 10.
 Catalysis results of various dienes and trienes with 5 mol% of octanethiolate-capped Pd nanoparticle in CDCl₃ at 1 atm H₂ after 24 h.

friendlier than other homogenous and heterogeneous catalysts tested for diene hydrogenation.

4. Conclusions

This chapter reviewed the use of various catalysts including metal complexes, supported metals and metal nanoparticles, colloidal nanoparticles for selective hydrogenation of polyunsaturated olefins, mostly dienes and trienes. Selective hydrogenation of polyenes has been considered as an important process in many chemical and pharmaceutical industries. By controlling chemical environments around active catalytic sites using organic ligands, inorganic dopants, ionic liquids, dendrimers, secondary metals, etc., the catalytic activity and selectivity of various catalysts for partial hydrogenation of polyenes could be improved. Especially, nanocatalyzed selective hydrogenation represents a rapidly growing field, but there is still much work to be done to generate industrially viable nanocatalysts that can be operated under many catalytic cycles with acceptable integrity. In addition, more in-depth understanding of critical structure–function relationships should be obtained for the development of optimized nanocatalysts with high chemoselectivity and stereoselectivity.

Acknowledgements

This research was funded by National Institute of General Medical Science [GM089562].

Conflict of interest

The authors declare no conflict of interest. The funding sponsor had no role in the design of the study, in the writing of the manuscript, and in the decision to publish the research results.


IntechOpen

Author details

Ting-An Chen and Young-Seok Shon*
Department of Chemistry and Biochemistry, California State University,
Long Beach, CA, USA

*Address all correspondence to: ys.shon@csulb.edu

IntechOpen

© 2018 The Author(s). Licensee IntechOpen. This chapter is distributed under the terms of the Creative Commons Attribution License (<http://creativecommons.org/licenses/by/3.0>), which permits unrestricted use, distribution, and reproduction in any medium, provided the original work is properly cited. 

References

- [1] Bond GC. Metal-Catalysed Reactions of Hydrocarbons. New York: Springer; 2005
- [2] Derrien ML. Studies in Surface Science and Catalysis. 1986;27:613
- [3] Erman WF. Chemistry of the Monoterpenes: An Encyclopedic Handbook. New York, NY: M. Dekker; 1985. p. 1709
- [4] Mimoun H. Catalytic opportunities in the flavor and fragrance industry. CHIMIA International Journal for Chemistry. 1996;50(12):620-625
- [5] Raoult Y, Choukroun R, Basso-Bert M, Gervais D. Hydrogenation and isomerization of olefins with diphenylphosphinomethyl hydride zirconium, $[\text{Cp}_2\text{ZrH}(\text{CH}_2\text{PPh}_2)]_n$, a selective homogeneous catalyst. Journal of Molecular Catalysis. 1992;72(1):47-58
- [6] Bond GC, Rawle AF. Catalytic hydrogenation in the liquid phase. Part 1. Hydrogenation of isoprene catalysed by palladium, palladium-gold and palladium-silver catalysts. Journal of Molecular Catalysis A: Chemical. 1996;109(3):261-271
- [7] Schrock RR, Osborn JA. Catalytic hydrogenation using cationic rhodium complexes. 3. The selective hydrogenation of dienes to monoenes. Journal of the American Chemical Society. 1976;98(15):4450-4455
- [8] Frankel EN, Butterfield RO. Homogeneous hydrogenation of diolefins catalyzed by tricarbonyl chromium complexes. I. Stereoselective 1,4-addition of hydrogen. The Journal of Organic Chemistry. 1969;34(12):3930-3936
- [9] Valentine D Jr, Johnson KK, Priester W, Sun RC, Toth K, Saucy G. Rhodium chiral monophosphine complex catalyzed hydrogenations of terpenic and .alpha.-(acylamino)-substituted acrylic acids. The Journal of Organic Chemistry. 1980;45:3698
- [10] Panella L, Feringa BL, de Vries JG, Minnaard AJ. Enantioselective Rh-catalyzed hydrogenation of enol acetates and enol carbamates with monodentate phosphoramidites. Organic Letters. 2005;7:4177
- [11] Takaya H, Ohta T, Sayo N, Kumobayashi H, Akutagawa S, Inoue S, et al. Enantioselective hydrogenation of allylic and homoallylic alcohols. Journal of the American Chemical Society. 1987;109:1596-1598
- [12] Liu J, Krajangsri S, Singh T, de Serriis G, Chumnanvej N, Wu H, et al. Regioselective iridium-catalyzed asymmetric monohydrogenation of 1,4-dienes. Journal of the American Chemical Society. 2017;139:14470-14475
- [13] Chang H, Phillips J. Catalytic synergism in physical mixtures of supported iron-cerium and supported noble metal for hydroisomerization of 1,3-butadiene. Langmuir. 1997;13:477-482
- [14] Sales EA, de Jesus Mendes M, Bozon-Verduraz F. Liquid-phase selective hydrogenation of hexa-1,5-diene and hexa-1,3-diene on palladium catalysts. Effect of tin and silver addition. Journal of Catalysis. 2000;195:96-105
- [15] Xu W, Ni J, Zhang Q, Feng F, Xiang Y, Li X. Tailoring supported palladium sulfide catalysts through H₂-assisted sulfidation with H₂S. Journal of Materials Chemistry A. 2013;1:12811-12817
- [16] Bachiller-Baeza B, Iglesias-Juez A, Castillejos-López E, Cuerrero-Ruiz A,

- Di Michiel M, Fernández-García M, et al. Detecting the genesis of a high-performance carbon-supported Pd sulfide nanophase and its evolution in the hydrogenation of butadiene. *ACS Catalysis*. 2015;5:5235-5241
- [17] Kahsar KR, Schwartz DK, Medlin JW. Selective hydrogenation of polyunsaturated fatty acids using alkanethiol self-assembled monolayer-coated Pd/Al₂O₃ catalysts. *ACS Catalysis*. 2013;3:2041-2044
- [18] Karakhanov E, Maximov A, Kardasheva Y, Semernina V, Zolotukhina A, Ivanov A, et al. Pd nanoparticles in dendrimers immobilized on silica-polyamine composites as catalysts for selective hydrogenation. *ACS Applied Materials & Interfaces*. 2014;6(11):8807-8816
- [19] Yi H, Du H, Hu Y, Yan H, Jiang HL, Lu J. Precisely controlled porous alumina overcoating on Pd catalyst by atomic layer deposition: Enhanced selectivity and durability in hydrogenation of 1,3-butadiene. *ACS Catalysis*. 2015;5:2735-2739
- [20] Bemsmeier D, Chuenchom L, Paul B, Rummeler S, Smarsly B, Kraehnert R. Highly active binder-free catalytic coatings for heterogeneous catalysis and electrocatalysis: Pd on mesoporous carbon and its application in butadiene hydrogenation and hydrogen evolution. *ACS Catalysis*. 2016;6:8255-8263
- [21] Hugon A, Delannoy L, Krafft JM, Louis C. Selective hydrogenation of 1,3-butadiene in the presence of an excess of alkenes over supported bimetallic gold-palladium catalysts. *Journal of Physical Chemistry C*. 2010;114:10823-10835
- [22] Zweni PP, Alper H. Silica-supported dendrimer-palladium complex-catalyzed selective hydrogenation of dienes to monoolefins. *Advanced Synthesis and Catalysis*. 2006;348(6):725-731
- [23] Yardimci D, Serna P, Gates BC. Tuning catalytic selectivity: Zeolite- and magnesium oxide-supported molecular rhodium catalysts for hydrogenation of 1,3-butadiene. *ACS Catalysis*. 2012;2:2100-2113
- [24] Speziali MG, Moura FCC, Robles-Dutenhefner PA, Araujo MH, Gusevskaya EV, dos Santos EN. Selective hydrogenation of myrcene catalyzed by complexes of ruthenium, chromium, iridium and rhodium. *Journal of Molecular Catalysis A: Chemical*. 2005;239(1-2):10-14
- [25] Robles-Dutenhefner PA, Speziali MG, Sousa EMB, dos Santos EN, Gusevskaya EV. Selective hydrogenation of myrcene catalyzed by sol-gel Pd/SiO₂. *Applied Catalysis A: General*. 2005;295(1):52-58
- [26] Luza L, Rambor CP, Gual A, Bernardi F, Domingos JB, Grehl T, et al. Catalytically active membrane like devices: Ionic liquid hybrid organosilicas decorated with palladium nanoparticles. *ACS Catalysis*. 2016;6(10):6478-6486
- [27] Niu Y, Crooks RM. Preparation of dendrimer-encapsulated metal nanoparticles using organic solvents. *Chemistry of Materials*. 2003;15(18):3463-3467
- [28] Ornelas C, Salmon L, Aranzaes JR, Astruc D. Catalytically efficient palladium nanoparticles stabilized by "click" ferrocenyl dendrimers. *Chemical Communications*. 2007;46:4946-4948
- [29] San KA, Shon Y-S. Synthesis of alkanethiolate-capped metal nanoparticles using alkyl thiosulfate ligand precursors: A method to generate promising reagents for selective catalysis. *Nanomaterials*. 2018;8:346. DOI: 10.3390/nano8050346

[30] Sadeghmoghaddam E, Gu H, Shon YS. Pd nanoparticle-catalyzed isomerization vs hydrogenation of allyl alcohol: Solvent-dependent regioselectivity. *ACS Catalysis*. 2012; 2(9):1838-1845

[31] Gavia DJ, Shon Y-S. Controlling surface ligand density and core size of alkanethiolate-capped Pd nanoparticles and their effects on catalysis. *Langmuir*. 2012;28(40):14502-14508

[32] Zhu JS, Shon Y-S. Mechanistic interpretation of selective catalytic hydrogenation and isomerization of alkenes and dienes by ligand deactivated Pd nanoparticles. *Nanoscale*. 2015;7(42): 17786-17790

[33] Chen T-A, Shon Y-S. Alkanethioate-capped palladium nanoparticle for selective catalytic hydrogenation of dienes and trienes. *Catalysis Science & Technology*. 2017;7:4823-4829. DOI: 10.1039/C7CY01880K